Importance of integrated results of different non-destructive techniques in order to evaluate defects in panel paintings: the contribution of infrared, optical and ultrasonic techniques

S. Sfarra*[a], P. Theodorakeas[b], C. Ibarra-Castanedo[c], N. P. Avdelidis[b], A. Paoletti[d], D. Paoletti[a], K. Hrissagis[b], A. Bendada[c], M. Koui[b], X. Maldague[c]

[a]Las.E.R. Laboratory, University of L'Aquila, Department of Mechanical, Management and Energy Engineering, Piazzale E. Pontieri 1, I-67100, Loc. Monteluco di Roio, Roio Poggio, L'Aquila (AQ), Italy;

[b]NDT Lab, National Technical University of Athens, School of Chemical Engineering, Department of Materials Science & Engineering, Iroon Polytechniou 9. Zografou Campus, 15780 Athens, Greece;

[c]Computer Vision and Systems Laboratory, Laval University, Department of Electrical and Computer Engineering, 1065, av. de la Médecine, Quebec City, Québec (QC), Canada;

[d]University of L'Aquila, Department of Mechanical, Management and Energy Engineering, Piazzale E. Pontieri 1, I-67100, Loc. Monteluco di Roio, Roio Poggio, L'Aquila (AQ), Italy

ABSTRACT

The increasing deterioration of panel paintings can be due to physical processes that take place during exhibition or transit, or as a result of temperature and humidity fluctuations within a building, church or museum. In response to environmental alterations, a panel painting can expand or contract and a new equilibrium state is eventually reached. These adjustments though, are usually accompanied by a change in shape in order to accommodate to the new conditions. In this work, a holographic method for detecting detached regions and micro-cracks is described. Some of these defects are confirmed by *Thermographic Signal Reconstruction* (TSR) technique. In addition, *Pulsed Phase Thermography* (PPT) and *Principal Component Thermography* (PCT) allow to identify with greater contrast two artificial defects in Mylar which are crucial to understand the topic of interest: the discrimination between defect materials. Finally, traditional contact ultrasounds applications, are widely applied for the evaluation of the wood quality in several characterization procedures. Inspecting the specimen from the front side, the natural and artificial defects of the specimen are confirmed. Experimental results derived by the application of the integrated methods on an Italian panel painting reproduction, called *The Angel specimen*, are presented. The main advantages that these techniques can offer to the conservation and restoration of artworks are emphasized.

Keywords: Infrared Thermography, Holographic Interferometry, Ultrasonic Testing, Panel Paintings, Defects.

1. INTRODUCTION

A panel painting is a painting made on a flat panel of wood, either a single piece, or a number pieces joined together. Until canvas became the more popular support medium in the 16th century, it was the normal form of support for a painting not on a wall (fresco) or vellum, which was used for miniatures in illuminated manuscripts and paintings for the framing. The technique is known to us through Cennino Cennini's *The Craftsman's Handbook (Il libro dell'arte)* published in 1390, and other sources.

It changed little over the centuries. It was a laborious and painstaking process: first of all, a carpenter would construct a solid wood piece the size of the panel needed. Usually a radial cut piece was preferred, with the outer sapwood excluded.

In Italy it was usually seasoned poplar, willow or linden. It would be planed and sanded and if needed, joined with other pieces to obtain the desired size and shape.

*stefano.sfarra@univaq.it; phone ++39 (0) 862 434350; fax ++39 (0) 862 431233; http://laser.ing.univaq.it/

Subsequently, the wood would be coated with a mixture of animal-skin glues and resin and covered with linen (the mixture and linen combination was known as a "size"). Finally, once the size has dried, layers of gesso are applied, each layer sanded down before the next applied, sometimes as many as 15 layers, before a smooth hard surface emerged, not unlike ivory. This stage was not done after the 16th century.

Once the panel construction as complete, the design was laid out, usually in charcoal. The usual ancient painting technique was encaustic: this uses heated wax as the medium for the pigments. This was replaced before the end of first millennium by tempera, which uses an egg-yolk medium.

Using small brushes dipped in a mixture of pigment and egg-yolk, the paint was applied in very small strokes. Because tempera (like encaustic) dries quickly and is not conducive to mistakes, each stroke had to be perfect each time. This exacting perfection shaped the nature and style of the art produced[1].

Panel paintings is one of the products of cultural heritage; hence its preservation is necessary for the continuation of the historical evolution of the human species. For this motive, art conservators need to constantly record the condition of objects and, if necessary, to apply methods and materials which stabilize their condition without affecting the integrity of the object. Therefore, a thorough understanding of the exact preservation condition is necessary. This can be achieved mainly by structural diagnosis techniques, which can offer unique information concerning structural evolving defects which are quite often not observed by other techniques. Structural diagnostics techniques can lead to the identification of specific areas object of immediate treatment and can also guide the conservator to the choice of proper methods and materials[2].

Structural diagnostics[3] is one of the main fields in the conservation of artwork[4,5]. A number of optical and related techniques are employed for the non-destructive investigation of panel paintings[6,7]. Holographic interferometry[8], infrared thermography[9,10] and ultrasonic techniques[11] have been used successful.

The focus of this paper is to use Holographic Interferometry, IR Thermography and Ultrasonic techniques as an integrated structural diagnostics tool to gain a complete information map about surface and subsurface defects of a wooden panel painting sample.

The sample is a realistic construction, as described in Section 2, to allow the investigation of measurement techniques in a controlled way on a test sample with similar characteristics to a real artwork.

1.1 Holographic Interferometry for nondestructive testing – Double Exposure (DE) method

Double-exposure holography is at present the most common and versatile method used in artwork diagnostics. Details of the technique can be found in literature[12,13]. Here we give a brief description of its application as nondestructive testing.

Two holograms are recorded on the same holographic plate, with each one capturing the object in a different state separated by a fixed time interval (Figure 1a and Figure 1b).

During the reconstruction the two waves, scattered by the object in its two states, will be reconstructed simultaneously and interfere, producing a three dimensional image of the object covered by a fringe pattern (Figure 1c).
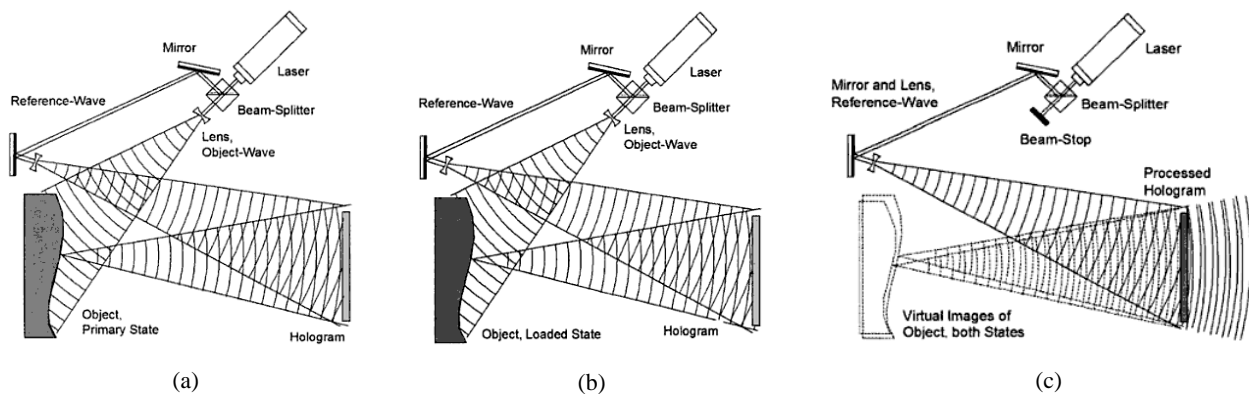

Figure 1. Recording (a), (b), and reconstruction (c) of a double exposure holographic interferogram[14].

This fringe pattern can be used to gain meaningful information with regard to the structural characteristics of an object, by observing the surface movement produced when it is subjected to stressing force.

As such, it offers the potential for many nondestructive inspections wherein the parameter of interest (e.g. cracks, voids, debonds, delaminations) can be made manifest as discontinuities in surface deformation. The discontinuities appear as an anomaly in an otherwise regular interferometric fringe pattern and hence enable the region of fault to be identified[14].

The stress must be chosen in such a way that the anomalies induce detectable perturbations in the surface deformation.

Usually a thermal stress obtained by heating the surface with an infrared lamp or a stream of moderately warm air, is chosen empirically with guidance provided by an analysis of anticipated deformation and by previous results obtained from programmed models.

On the basis of calibration experiments, it is reasonable to assume that the fringes will generally have a higher spatial density in regions of a structure where strain concentrations are present.

Furthermore, one would expect fringe irregularities to exist in regions of uneven load distribution.

1.2 Pulsed Phase Thermography (PPT)

Pulsed phase thermography (PPT)[15,16] is an attractive technique, in which data is transformed from the time domain to the frequency domain using the one-dimensional discrete Fourier transform (DFT):

$$F_n = \Delta t \sum_{k=0}^{N-1} T(k\Delta t)\exp^{(-j2\pi nk/N)} = \mathrm{Re}_n + j\,\mathrm{Im}_n$$
(1)

where j is the imaginary number ($j_2 = -1$), n designates the frequency increment ($n = 0, 1, ... N$), Δt is the sampling interval, and R_e and I_m are the real and the imaginary parts of the transform, respectively. In this case, real and imaginary parts of the complex transform are used to estimate the amplitude A, and the phase ϕ[17]:

$$A_n = \sqrt{\mathrm{Re}_n^2 + \mathrm{Im}_n^2} \qquad\qquad \phi_n = \tan^{-1}\left(\frac{\mathrm{Im}_n}{\mathrm{Re}_n}\right)$$
(2)

The DFT can be used with any wavefront (e.g. transient pulsed thermographic profiles).
Phase profiles for surface temperature are anti-symmetric, providing redundant information in both sides of the frequency spectra. In the following, only the positive part of the frequency spectra is used whilst the negative frequencies can be safely discarded. The phase is of particular interest in NDE given that is less affected than raw thermal data by environmental reflections, emissivity variations, non-uniform heating, and surface geometry and orientation. These phase characteristics are very attractive not only for qualitative inspections but also for quantitative characterization of materials.
For instance, a depth inversion technique using the phase from PPT has been proposed[18,19].
The technique relies on the thermal diffusion length equation, i.e. $\mu=(\alpha/\pi{\cdot}f)^{1/2}$, in a manner similar to lock-in thermography[17].
Nevertheless, as it well-known[20], noise content in phase data is considerable, especially at high frequencies. This cause a problem for the determination of the blind frequency[21].
A de-noising step is therefore often required.
The combination of PPT and TSR (discussed in the next paragraphs) has proven to be very attractive for this matter, reducing noise and allowing the depth retrieval for a defect[22].
Another difficulty is that, given the time-frequency duality of the Fourier transform, special care must be given to the selection of the sampling and truncation parameters prior to the application of the PPT. These two parameters depend on the thermal properties of the material and on the depth of the defect, which are often unknown. An interactive procedure has been proposed[23].
Data acquisition is fast and straightforward, as illustrated in Figure 2.
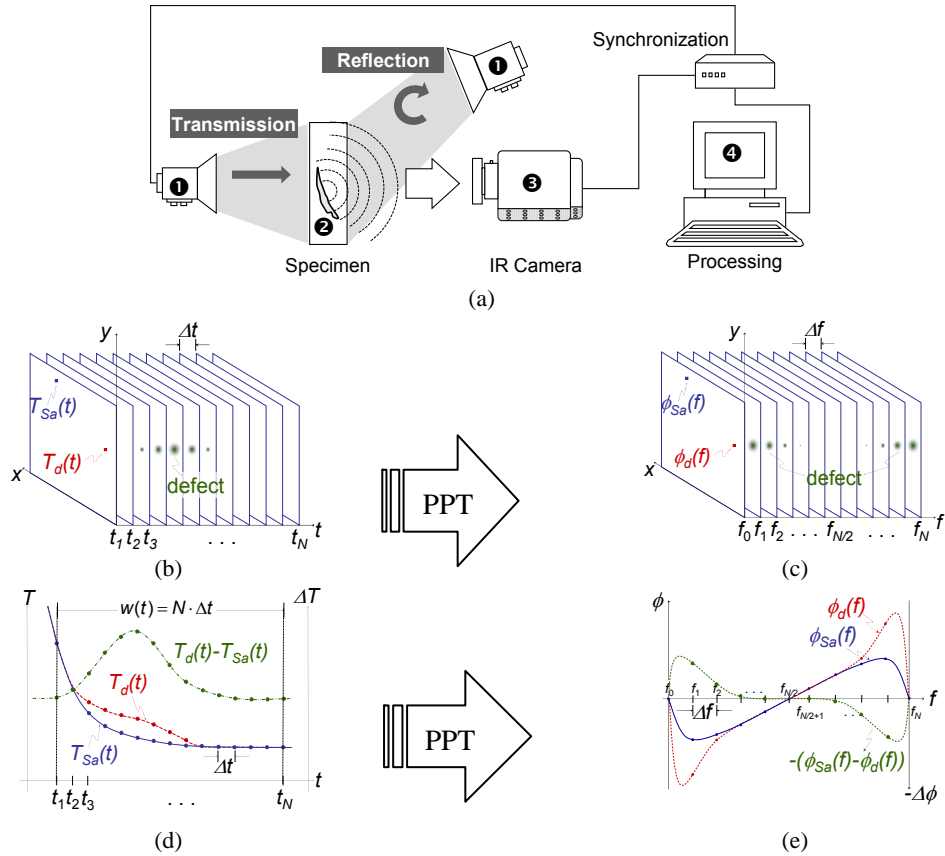
Figure 2. Data acquisition and signal processing in PPT: (a) four steps for data acquisition, (b) thermogram 3D matrix depicting the appearance and disappearance of a defect through time, (c) phasegram 3D matrix showing the defect visibility in the frequency spectrum, (d) thermal profiles for a defective pixel (-T_d), a non-defective pixel (--T_{Sa}) and the difference between them (---T_d -T_{Sa}), and (e) phase profiles for a defective pixel (-ϕ_d), a non-defective pixel (--ϕ_{Sa}) and the difference between them (---ϕ_d -ϕ_{Sa}).

1.3 Thermographic Signal Reconstruction (TSR)

In subsurface defect detection, contrast and quality of the thermal data captured is critical. Low contrast image and noisy image may hide the revelation of subsurface defect. The most promising technique is for noise reduction is thermographic signal reconstruction (TSR) which is recently developed by Shepard's group in 2001[24] and got patented in 2003[25]. The algorithm of TSR is presented as follows.

This method implemented a well-known relationship that when a think solid sample is heated up, the surface response to the instantaneous uniform heating is described by the one-dimensional diffusion equation. The equation is applied in the assumption that the lateral diffusion components are nearly cancelled in a defect-free sample. When there are subsurface defects in the sample, the incident heat flow from the sample surface is impeded and hence the one-dimensional heat diffusion equation does not hold locally. Therefore, it can be said that when there are defects, the one-dimensional diffusion principal breaks down. Cooling of normal and anomalies will be separated and hence identification on defects can be easily made. Time evolution of the surface temperature in the logarithmic domain after responded to pulse heating is as follows:

$$\ln(T) = \ln\left(\frac{Q}{e}\right) - \frac{1}{2}\ln(\pi t)$$

(3)

Nowadays, the industry is looking for more convenient and fast methods for detection of smaller and deeper defects. Therefore, reconstructions of data sequences are developed for investigation since it facilitates the creation of time-derivative images. Normally, an experimental data is excellently fit into a polynomial equation as shown in the following:

$$\ln[T(t)] = \sum_{n=0}^{N} a_n [\ln(t)]^n \qquad (4)$$

A low-order expansion is applied intentionally as a low-pass filter which preserves the essential thermal response. Low-pass filter is applied since there should be no sudden jump in thermal energy. Once the raw data fitted into Equation (4), it can be reconstructed, since:

$$T(t) = \exp\left(\sum_{n=0}^{N} a_n [\ln(t)]^n \right) \qquad (5)$$

Besides noise reduction, another advantage of TSR method is that it facilitates creation of derivative image without adding additional noise contributions[26]. The major advantage of TSR derivative image is it shows apparent reduction of diffusion blurring since derivative images provide earlier indications of the presence of subsurface defect than normal contrast images on the same target. Time-derivatives processing enhance the detectability of the defect by increasing the signal-to-background contrast. The derivatives thermograms are much more sensitive to small changes in temperature amplitude than raw signal. In time-derivative analysis, each pixel time history is differentiated using the following expression[26]:

$$\frac{d\ln(T)}{d\ln(t)} = \sum_{n=0}^{N} n a_n \ln(t)^{n-1} \qquad (6)$$

Given that diffusion blurring has increasing influence on the observation of subsurface defect in the time sequence, therefore, blurring effect can be reduced with the possible earlier indication of the presence of defects. In addition, problems such as non-uniform heating, emissivity variations, environmental reflections and surface geometry have a great impact on raw thermal data[27]. In time derivative thermo sequence, the indication of defects will appear darker and then lighter than the intact region because the heat trapped above the defect slows down the cooling of the surface. However, it will eventually cool down more rapidly than the intact region at the later stage. Besides reducing the diffusion blurring effects, time-derivatives processing is also capable to reduce the influence of uneven heat distribution since the time derivative image is considering the temperature change instead of temperature amplitude. The following illustration (Figure 3) describes the relationship of first and second derivatives temperature decay curve to contrast curve.
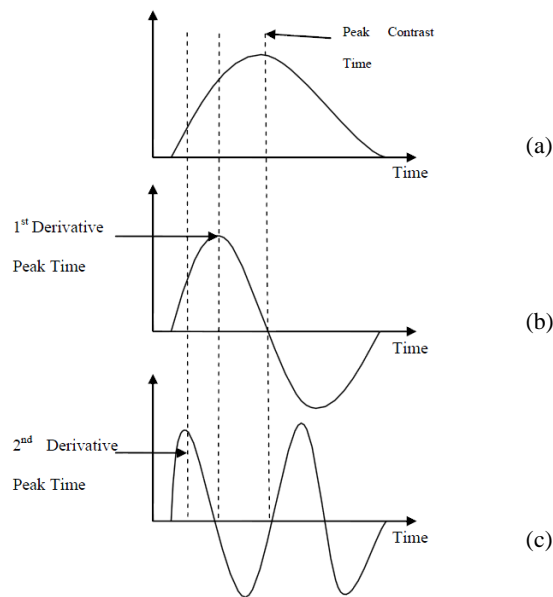

Figure 3. (a) Temperature contrast curve, (b) 1st and (c) 2nd derivative curve.

As shown in Figure 3, second derivative peak time is always shown first and followed by first derivative peak time and lastly the maximum contrast peak. It means that second derivative image gives the earliest indications of the presence of a subsurface defect compared with the temperature contrast image. The initial inflection point in the temperature contrast curve of a pixel corresponds to the peak of second derivative curve[28].

1.4 Ultrasonic Testing (UT)

In last years great efforts have been made on the development of measurement and testing techniques for wood and wooden structures with the aim of predicting their characteristics and ensuring their performances: particular attention has been devoted to ultrasonic measurement.

However, wood is a naturally grown, anisotropic and heterogeneous material that makes the use of ultrasonic measurement systems very challenging. In fact several parameters, e.g. the wood fibers disposition and the humidity content, can make the ultrasonic signals complex and difficult to be analyzed. These is even more difficult in the study of panel paintings where there is a complexity of materials and layers. Nevertheless Non Destructive Techniques (NDT), mostly based on traditional contact ultrasounds application, have been widely applied in the evaluation of the wood quality in several characterization procedures, for diagnostic purposes and for the classification in working conditions[29,30]. The developed experimental set-up is shown in Figure 4. The system is composed of two sensors: T is the transducer and R is the receiver. The transducer is stable, while the receiver is moved during each testing on the lines marked on the *Angel* specimen (Figure 10b).
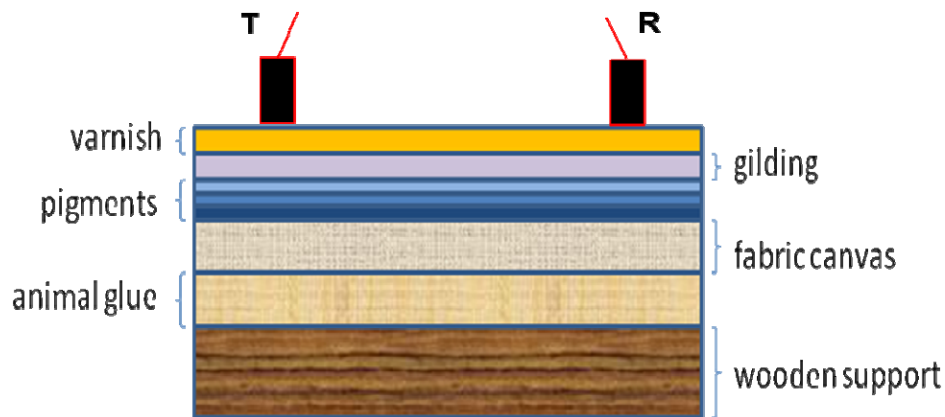

Figure 4. Scheme of the measurement system, UT (T: transducer, R: receiver) and cross-section of the artificially-made sample. The stratigraphy follows the typical one of the Cennino Cennini's painting.

For ultrasonic measurements, V- Meter MK III was used (Figure 10a). The measurements carried out with the higher frequency 2 M z, to bruit ultrasound waves in a small depth and identify the natural and artificial defects (A, B, C, D).

While the results of the interaction of the sound with flaws can also be displayed as an ultrasonic image, a more common type of display used in industrial inspections is a received voltage versus time trace, $V_R (t)$, on an oscilloscope, called an A-scan for a typical ultrasonic NDE flaw inspection system.

Since images are generated by processing combinations of such A-scans, A-scan data provides the fundamental basis for describing the output of industrial ultrasonic systems.

The basic components of the ultrasonic inspection system are the pulser/receiver, the cabling, the transducers, and the acoustic/elastic wave propagation and scattering processes present. The pulser section of the pulser/receiver generates short electrical pulses which travel through the cabling to the transmitting transducer.

The transducer converts these electrical pulses into acoustic pulses at its acoustic output port. In the setup shown in Figure 4, the sound beam is transmitted into the solid component being inspected and the beam interacts with any flaws that are present.

The flaw generates scattered wave pulses traveling in many directions, but some of these pulses reach the receiving transducer which then converts them into electrical pulses.

These electrical pulses travel again through cabling to the receiver section of the pulser/receiver, where they are amplified and displayed as a received A-scan voltage, $V_R\,(t)$, as a function of the time t^{31}.

2. SAMPLE CONSTRUCTION

The structural diagnosis of panel paintings is a procedure which investigates complex systems of materials and defects that in many cases are not visible to the naked eye. To develop structural diagnostic techniques, artificial samples that simulate original objects are required (Figures 4 and 5).

The protocol of construction was based on the traditional techniques described by the famous art masters of the time, such as Cennino Cennini[32,33]. Additionally, the study of the most typical defects found on panel paintings led to the selection of the ones chosen for the construction of the model sample.

In our specimen, the adhesion loss between the preparation layer and the painting film caused a particular configuration called *craquelure*[34]. *Craquelure*, in the first step, are diffuse microcracks that affected the *Angel* specimen (Figure 6b – defects E, F, G, H, I, L).

Detached regions were simulated by inserting a Mylar sheet (defect B) and a thin sponge covered with Mylar (defect D) at different depths. Figures 6c,d and 8a,b provide a useful indication of the different nature of the defects composition.

Unfortunately, the information about the exact depths of the defects has been lost.
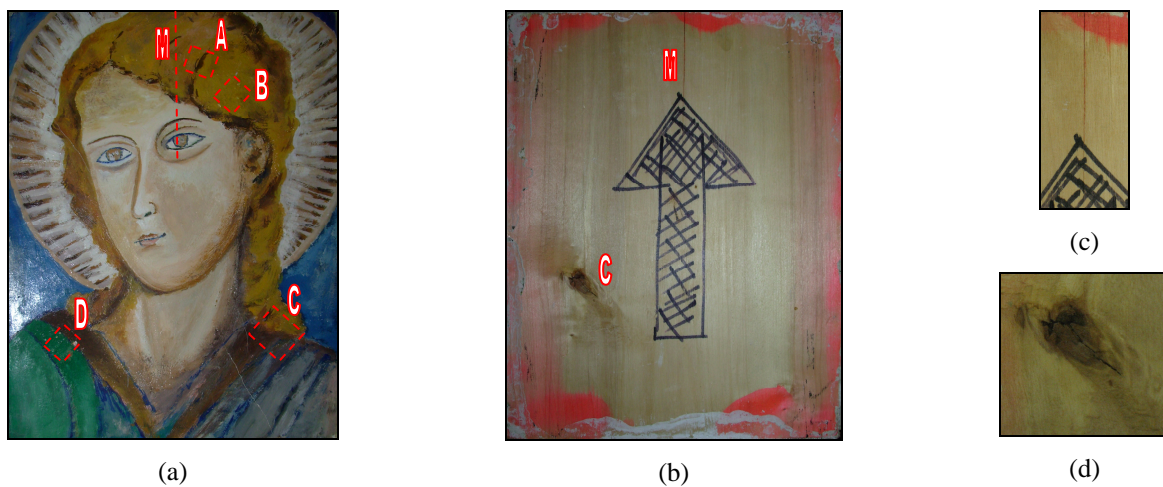

(a)   (b)   (c)   (d)

Figure 5. The Angel specimen and approximate location of the defects (except for the *craquelure*): (a) front side, (b) back side, (c), magnification of the M defect (crack) (d) magnification of the C defect (knot).

3. COMPARATIVE RESULTS

The wooden panel painting described in Section 2 was analyzed using the holographic interferometry, infrared thermography and ultrasonic techniques.

The specimen, consists of a 20 x 25 x 2 cm panel of poplar wood, with cracks inside the layered structure (defect M as seen in Figure 5c) or closer to the surface (defects E, F, G, H, I and L – *craquelure* – shown in Figure 6b), artificially detached regions (defects B and D – Figure 5a) and natural defects such as a knot (defect C – Figures 5 a,b,d) or a *satellite* defect due to longitudinal warping (defect A in Figure 5a).

Wood from trees of this genus (*Populus*) are light in color and light in weight. In Europe that of the white poplar (*P. canescens*) and the Lombardy poplar (*P. fastigata*) are the principal sources of timber poplar.

Poplar wood is soft, weak, fine-grained and fine-textured, it is diffuse-porous and the pores are very small.

The annual rings are fairly well defined but the rays are very fine and are not visible without a lens. Poplar was frequently used in the Italian schools for panel painting[35,36]. This is confirmed by our work.
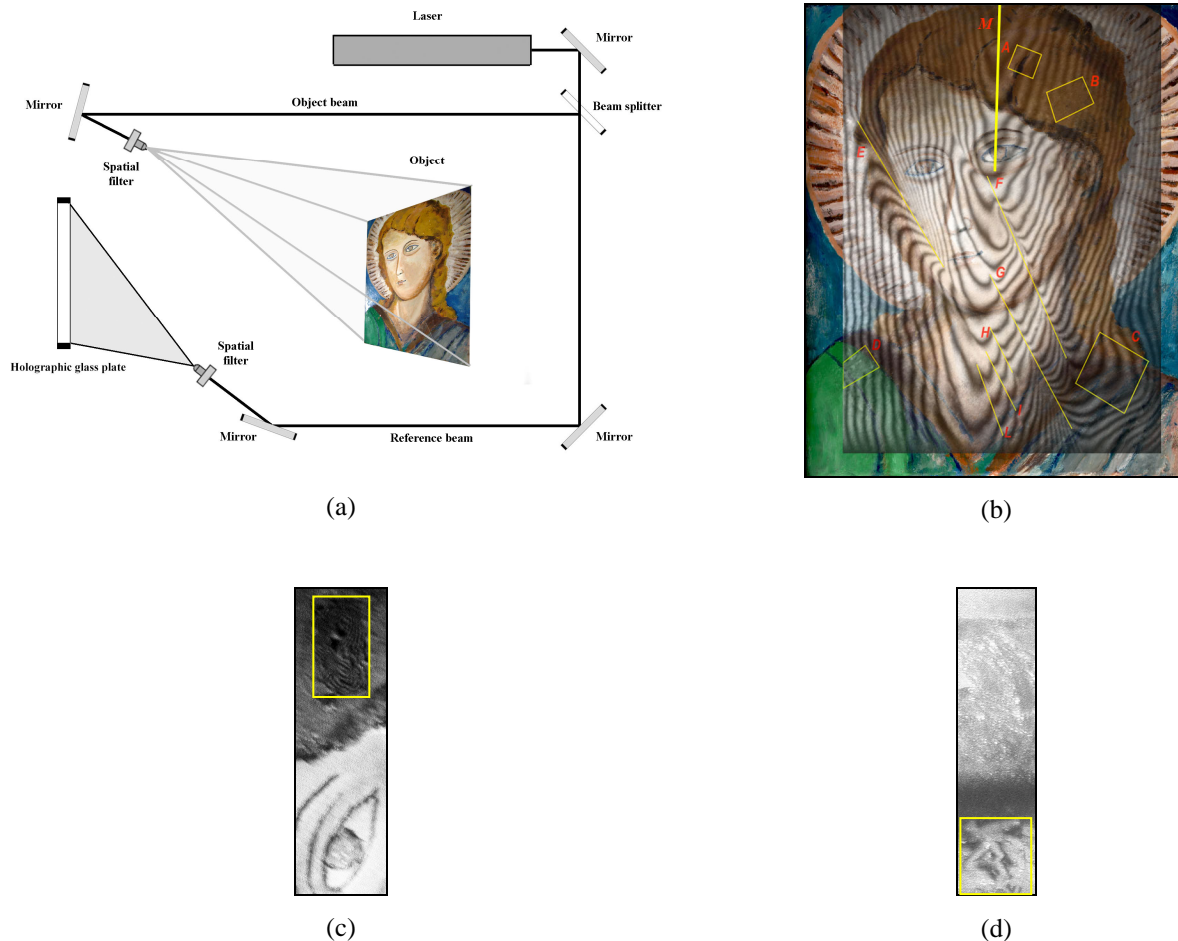
(a)

(b)

(c)

(d)

Figure 6. (a) Experimental setup for Double-Exposure HI, (b) overlap between three layers: visible image of the Angel specimen, HI – DE result and defects map, (c) magnification of the defect B from a second experiment, (d) magnification of the defect D from a second experiment.

The first step is to use holographic interferometry in the DE method, to determine regions of interest for subsequent detailed investigation with IR thermography and ultrasonic techniques. The classical set-up for holograms recording in DE is illustrated in Figure 6a. A disadvantage of double-exposure holographic interferometry is that information on intermediate states of the object is not available, but the experience of the research group that uses this technique may be able to compensate this difficulty in order to display all the flaws in an interferogram, as shown in Figure 6b. This interferogram was obtained after stressing the specimen with a 150 W IR lamp during 60 s at approximately 1 m of distance from the front of the object and using a laser with a power of 250 mW. The fabricated and natural defect locations are highlighted for reference. Two disbonds above the left ear and right shoulder can be clearly identified and a magnification, coming from a second set of experiments (150 W IR lamp during 90 s at approximately 1 m of distance), is presented in Figure 6c and in Figure 6d.

Defect C, due to the presence of a knot in the wood (Figure 5d), although less evident, is still in relief as seen in Figure 6b. Finally it is difficult to obtain a clear signature for defect A from this interferogram, it is probably located too deep and too small, to produce a strong enough detectable signal. Given the importance of *satellite* defects, interested readers may consult the Reference[37]. Very interesting to note the difference in signal produced by the depth crack (defect M – Figure 5c and Figure 6b) which emphasizes the broad cusps, from the surface and subsurface cracks (*craquelure* E, F, G, H, I, L – Figure 6b) with very narrow cusps.

For confirming these results, the *Angel* specimen was inspected by active thermography using a set of two 250 W lamps and a long-wave camera (FLIR S65 HS, 7.5-13 μm, 320x256 pixels).

The specimen was heated during 90 s and the surface cooling down was recorded during 180 s, providing 270 thermograms to process. Figure 7 shows selected results obtained by PPT.

Results in the first row were obtained by processing the heating phase exclusively, i.e. the 90 s. In Figure 7a, defect C can be slight seen and disappears in Figure 7b where appear the fabricated defects B and D.
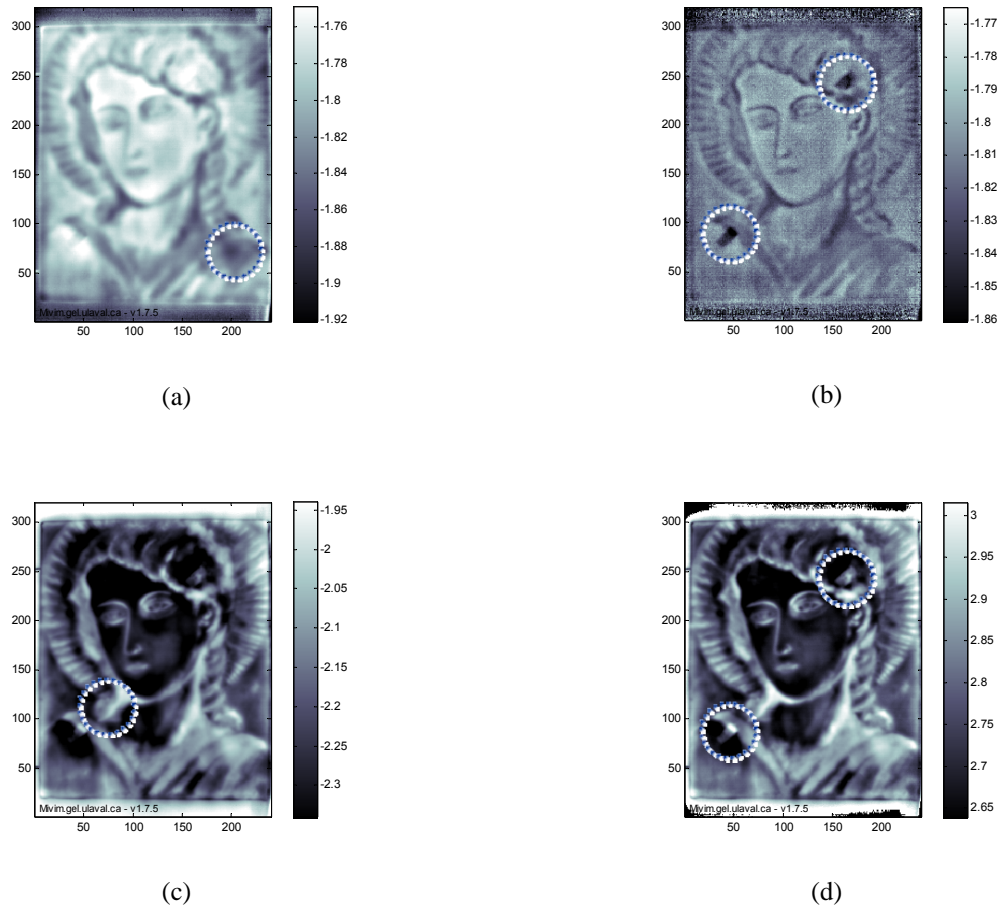

(a)

(b)

(c)

(d)

Figure 7. Selected PPT results. <u>First row</u>, obtained by processing the heating sequence exclusively (first 90 s): (a) f = 11.1 MHz, (b) f = 55.6 MHz. <u>Second row</u>, using the whole sequence (90 s heating + 180 s cooling): (c) f = 3.7 MHz, (d) f = 7.4 MHz.

Lastly, the second row presents the results obtained by processing the complete sequence, heating and cooling, i.e. 270 s.

Defects can be seen with good contrast in Figure 7d.

Interestingly, Figure 7c provides an indication of a geometrical figure (square shaped), similar to a buried defect.

Data was also processed using Principal Component Thermography (PCT) where the thermographic data is projected from its original space to its eingenspace to increase its variance and reduce its covariance so as to identify patterns in the data[38].

The PCA utilizes empirical orthogonal functions to establish statistical modes that highlight the variability within the thermograms spatially and temporally. PCT can be implemented mathematically through direct or Single Value

Deposition calculation routes. The use of this technique can confirm the different nature of defects[39] B and D and integrate the result obtained by holographic interferometry.

In fact, EOFs in Figure 8a and in Figure 8b were obtained by processing the complete sequence and are interesting and surprising since defect B, in Figure 8a, is clearly seen as a light area (as in the PPT phasegrams of Figure 7c,d) while defect D appears as dark area (contrary to the PPT phasegrams of Figure 7c,d); instead, in Figure 8b the dark and light area are reversed.

This can be useful to differentiate between internal defects.

(a)

(b)

Figure 8. Selected PCT results obtained by processing the whole sequence. (a) EOF2 (b) EOF4.

Subsequently, the specimen was tested with an integrated thermographic system (Voyage IR^{TM}) in order to confirm the cracks detected by holographic interferometry (Figure 6b). The data acquisition was performed with the use of a Long wave infrared camera (ThermaCAM^{TM} SC640 operating from 7.5 to 13.5 μm) of FPA type with image resolution 640x680 pixels (0.65 m rad) and thermal sensitivity 60 Mk at 30 °C, working on the maximum frequency of 30 Hz. The thermal stimulation was performed with the use of a heat gun (incorporated in the thermographic system) providing energy of 1875 Watt. The inspection of the specimen took place in reflection mode. The data obtained was processed using TSR approach (Mosaiq 4.0 software). Two of the surface cracks (E and G shown in Figure 6b) can be observed by extracting the first time and second time derivative images from the raw thermographic data, furthermore two artificial defects B and D can be perfectly seen (Figure 9).

(a)

(b)

Figure 9. First time derivative image (left) at t=2.6 s and second time derivative image (right) at 5.2 s in the 150 s heating procedure and working on the frame rate of 30 Hz.

The *Angel* specimen was investigated using lower frame rates in order to confirm the existence of the internal defects A and C in deeper layers of the painting, but no good results were observed. Finally, some testing was performed in the rear side of the sample with similar results. The specimen was finally investigated from its front side following four sets of

measurements (Figure 10a,b), using ultrasound technique in order to identify the artificial defects (B and D) and the natural defects (A and C).

(a)   (b)
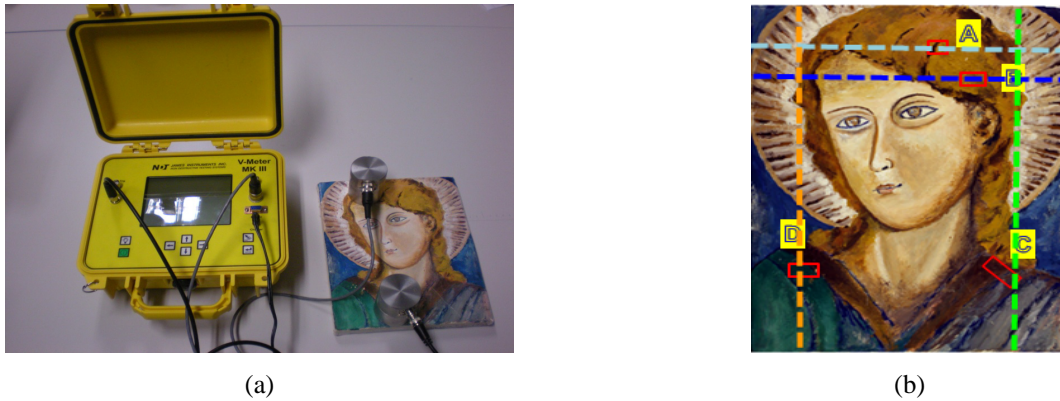
Figure 10. (a) Test arrangement for the ultrasound measurements, (b) sets of ultrasound measurements for the identification of hidden defects.

In Figure 11a a graphic representation of the set of measurements on the surface of the *Angel* specimen following the light blue line, is shown. The modification of the graphic line shows two different ranges where the line gradient changes due to the change of the ultrasonic speed during its penetration through the material of different composition. Namely, in the first range, the ultrasonic speed is 743 m/s and the change of the gradient is attributed to the presence of a *satellite* defect probably caused by the crack M (A defect). In the second part, the ultrasonic speed is 491 m/s. Similar results were observed for the identification of the others defects (B, D inclusions and C knot). In Figure 11b and 11c the graphic representations of the blue and green lines are shown respectively. The modification of the graphic lines shows two different ranges as well. The orange set of measurements represents the experimental result obtained for the defect D: in this graphic representation (Figure 11d) is as well observed a second line gradient change due to the complexity of the inclusion consists of sponge covered with Mylar.
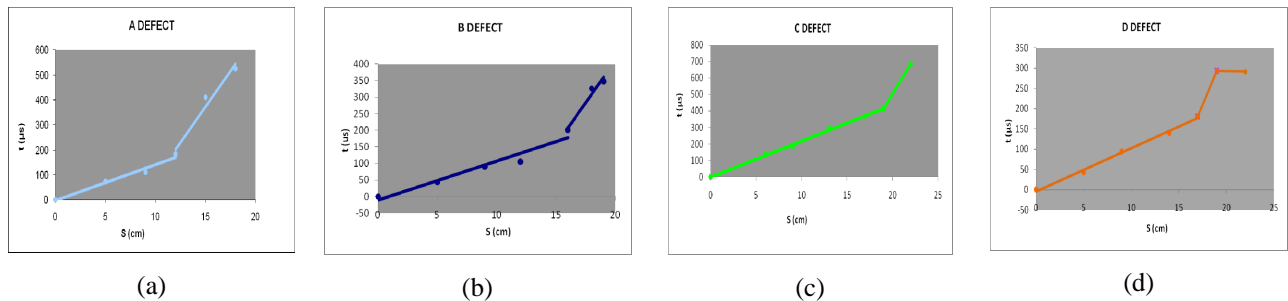

(a)   (b)   (c)   (d)

Figure 11. Graphic representations of the ultrasonic measurements.

4. CONCLUSIONS

The most established sector for the application of non destructive diagnostic techniques (NDT) is the industrial one, where they are widely used for checking products performance, maintenance and monitoring. On the other side, the employment of NDTs is still expanding in the field of Cultural Heritage (CH); this field is particularly eager of this type of technology and its use is increasing day after day. Material analysis, construction techniques and assessment of conservation state are complex activities, so that technicians working with CH are well aware of the importance of the techniques that may help them to increase the knowledge level of these issues.

Of course, it is of great importance to proceed with a well structured frame of data collection and interpretation; the mistrust that some restorers deserve to in situ and laboratory tests depends also on the fact that sometimes diagnostic technicians work independently from them, making their own work and results not-shareable.

To avoid this, it is highly advisable to create a group composed of different experts coming from different fields, as in this work, that jointly agree where to make measurements, using which techniques and methodologies, and how to read measurements results. This manuscript demonstrates the potential advantages of using both Holographic Interferometry, IR Thermography and Ultrasonic Techniques for structural diagnostics of wooden panel painting.

HI provides the surface, and sub-surface information about the object and in some cases, can be combined with thermographic PCT method, and ultrasonic technique, to identify the nature of subsurface defects. Thermographic TSR method can be helpful in confirming the presence of *craquelure* highlighted by DE method (defects E, F, G, H, I, L).

PPT phasegram at f=11.1 MHz it was found useful in identifying a natural defect such as a loose knot (defect C) besides confirming the presence of two artificial inclusions (defects B and D). Of crucial importance was the application of ultrasonic technique especially for the defect A (*satellite* defect) identified by HI.

More research is needed through to fully understand how to integrate the results obtained by HI on the depth crack M and for understanding the nature of the subsurface defect, detected by thermographic PPT method at f=3.7 MHz.

REFERENCES

[1] [online] http://en.wikipedia.org/wiki/Panel_painting, accessed on March 2011.
[2] Groves, R.M., Pradarutti, B., Kouloumpi, E., Osten W. and Notni, G. , "2D and 3D non-destructive evaluation of a wooden panel painting using shearography and terahertz imaging," NDT&E International 42(6), 543-549 (2009).
[3] Fotakis, C., Anglos, D., Zafiropulos, V., Georgiou S. and Tornari, V., "Laser interferometry for direct structural diagnostics", Lasers in the preservation of cultural heritage, principles and applications, CRC Press, Boca Raton, 125-182 (2007).
[4] Fotakis, C., Anglos, D., Zafiropulos, V., Georgiou S. and Tornari, V., Lasers in the preservation of cultural heritage, principles and applications, CRC Press, Boca Raton, 1-336 (2007).
[5] In: Castillejo, M., Editor, Lasers in the conservation of artworks, CRC Press, Leiden, 1-512 (2008).
[6] Paoletti, D., Schirripa Spagnolo, G., Facchini M. and Zanetta, P., "Artwork diagnostics with fiber-optic digital speckle pattern interferometry," Appl. Opt. 32, 6236-6241 (1993).
[7] Tornari, V., Bonarou, A., Castellini, P., Esposito, E., Osten W. and Kalms M.K. et al., "Laser-based systems for the structural diagnostic of artwork: an application to XVII-century Byzantine icons," Proc SPIE 4402, 172-183 (2001).
[8] Paoletti, D., and Schirripa-Spagnolo, G., "Interferometric methods for artwork diagnostic," Progress in Optics XXXV, 197-255 (1996).
[9] Maldague, X.P.V., Jones, T.S., Kaplan, H., Marinetti, S. and Pristay, M., Nondestructive Handbook, "Infrared and Thermal Testing", 3, X. Maldague technical ed., P. O. Moore ed., 3rd edition, Columbus, Ohio, ASNT Press, 1-718 (2001).
[10] Ibarra-Castanedo, C., Sfarra, S., Ambrosini, D., Paoletti, D., Bendada A. and Maldague, X., "Infrared vision for the nondestructive assessment of panel paintings," CINDE Journal 31(5), 5-9 (2010).
[11] Siddiolo, A.M., D'Acquisto, L., Maeva, A.R. and Maev, R.G., "Wooden panel paintings investigation: an air-coupled ultrasonic imaging approach," IEEE transactions on ultrasonic, ferroelectrics and frequency control 54(4), 836-846 (2007).
[12] Stetson, K.A., "A critical review of hologram interferometry", In: Holography, Proceedings of the meeting, Los Angeles, 14-35 (1985).
[13] Heslehurst, R.B., "A review of holographic interferometry investigations of defects and damage in composite materials", Journal of Advanced Materials 41, 5-12 (2009).
[14] Kreis, T., "Handbook of holographic interferometry – Optical and digital methods", Wiley, Germany, 1-554 (2005).
[15] Maldague, X.P. and Marinetti, S., "Pulse Phase Infrared Thermography", J. Appl. Phys., 79(5), 2694-2698 (1996).
[16] Ibarra-Castanedo, C. and Maldague, X., "Pulsed Phase Thermography Reviewed", QIRT J., 1(1), 47-70 (2004).
[17] Meola, C. and Carlomagno, G.M., "Recent Advances in the Use of Infrared Thermography", Meas. Sci. Technol., 15, 27–58 (2004).

[18] Ibarra-Castanedo, C., "Quantitative subsurface defect evaluation by pulsed phase thermography: depth retrieval with the phase," *Ph. D. thesis*, Université Laval, [available online: http://www.theses.ulaval.ca/2005/23016/23016.pdf] (2005).

[19] Ibarra-Castanedo, C., Avdelidis, N. P., Grinzato, E. G., Bison, P. G., Marinetti, S., Liu, C. Genest, M. and Maldague, X. P. "Quantitative inspection of non-planar composite specimens by pulsed phase thermography," Qirt Journal, 3(1), 25-40 (2006).

[20] Couturier, J-P. and Maldague, X., "Pulsed Phase Thermography of Aluminum Specimens", Proc. SPIE, 3056, 170-175 (1997).

[21] Ibarra-Castanedo, C., Sfarra, S., Ambrosini, D., Paoletti, D., Bendada, A. and Maldague, X., "Subsurface defect characterization in artworks by quantitative pulsed phase thermography and holographic interferometry", QIRT Journal, 5(2), 131-149 (2008).

[22] Ibarra-Castanedo, C., Genest, M., Servais, P., Maldague, X. and Bendada, A., "Qualitative and quantitative assessment of aerospace structures by pulsed thermography," NDT & E, 22(2 and 3), 199-215 (2007).

[23] Ibarra-Castanedo, C. and Maldague, X. "Interactive methodology for optimized defect characterization by quantitative pulsed phase thermography", Research in Nondestructive Evaluation, 16(4), 1-19 (2005).

[24] Shepard, S.M., Ahmed, T., Rubadeux, B.A., Wang D. and Lhota J.R., "Synthetic processing of pulsed thermographic data for inspection of turbine components", Insight 43(9), 587-589 (2001).

[25] Shepard, S.M., "Temporal noise compression and analysis of thermographic image data sequences", US Patent 6516084 (2003).

[26] Shepard, S.M., Lhota, J.R., Rubadeux, A., Wang, D. and Ahmed T., "Reconstruction and Enhancement of active thermographic image sequences", Optical Engineering 42, 1337-1342 (2003).

[27] Maldague, X. P. V., "Theory and practice of infrared technology for nondestructive testing", John Wiley & Sons, N. Y., 1-500 (2001).

[28] Sham Fung Chu, J., "Studies of using infrared flash thermography (FT) for detection of surface cracks, subsurface defects and water-paths in building concrete structures" *Master of Philosophy*, City University of Hong Kong, [available online: http://lbms03.cityu.edu.hk/theses/ftt/mphil-meem-b23405582f.pdf] (2008).

[29] Sandoz, J.L., Benoit, Y., Demay, L., "Wood testing using acousto-ultrasonic technique", Proceedings of the 12th International Symposium on Nondestructive testing of Wood, University of Western Hungary, Sopron, 97-104 (2000).

[30] Saporiti Machado, J., Costa, D., Cruz, H., "Evaluation of pine timber strength by drilling and ultrasonic testing", International Symposium on nondestructive testing in civil engineering, Berlin, CD-ROM (2003).

[31] Shmerr, L.W., Jen, C.K., Kobayashi, M., et al. "Ultrasonic and advanced methods for nondestructive testing and material characterization", Chen C.H. ed., Singapore, World scientific publishing Co. Pte. Ltd., 1-665 (2007).

[32] Moutsatsou, A.P., Trompeta, M., Olafsdottir, J., Tsaroucha, C., Terlixi, A.V., Groves, R.M., et al., "Laser-based structural diagnosis: a museum's point of view", Lasers in the conservation of artworks, Leiden, CRC Press, 407-411 (2008).

[33] Ibarra-Castanedo, C., Sfarra, S., Ambrosini, D., Paoletti, D., Bendada, A., Maldague, X., "Diagnostics of panel paintings using holographic interferometry and pulsed thermography", QIRT Journal, 7(1), 85-114 (2010).

[34] Abas, F.S. and Martinez, K., "Craquelure analysis for content-based retrieval", in 14th International conference on digital signal processing, Santorini, Greece, 111-114 (2002).

[35] Gettens, R.J. and Stout G.L., "Painting Materials – A schort encyclopaedia", Dover Publications Inc., N.Y., 1-333 (1966).

[36] Cennini, C., Il libro dell'arte, revised edition, Vicenza, Neri Pozza (2003), The Craftsman, English translation by Daniel V. Thompson Jr. N.Y., Dover, 5-6 (1971).

[37] Sfarra, S., Ambrosini, D., Paoletti, A., Paoletti, D., Ibarra-Castanedo, C., Bendada, A., Maldague, X., "Quantitative infrared thermography (IRT) and holographic interferometry (HI): non destructive testing (NDT) for defects detection in the silicate ceramics industry", Advances in Science and Technology, 68, 102-107 (2010).

[38] Rajic, N., "Principal component thermography", DSTO Aeronautical and Maritime Research Laboratory Technical Report TR-345 (2002).

[39] Sfarra, S., Bendada, A., Paoletti, A., Paoletti, D., Ambrosini, D., Ibarra-Castanedo, C. and Maldague, X., "Square Pulse Thermography (SPT) and Digital Speckle Photography (DSP): non destructive techniques (NDT) applied to the defect detection in aerospace materials", in 2nd International Symposium on NDT in Aerospace. Hamburg, Germany, (CD-ROM) (2010).